Published in final edited form as:
Nanomedicine. 2013 November ; 9(8): 1235–1244. doi:10.1016/j.nano.2013.05.010.

A comprehensive analysis of transfection-assisted delivery of iron oxide nanoparticles to dendritic cells

Shinji Toki, PhD[a], **Reed A. Omary, MD**[b,c,e], **Kevin Wilson, MS**[b,c], **John C. Gore, PhD**[b,c,d,h], **R. Stokes Peebles Jr., MD**[a,*], and **Wellington Pham, PhD**[b,c,d,e,f,g,*]

[a]Division of Allergy, Pulmonary and Critical Care Medicine, Vanderbilt School of Medicine, Nashville, TN, USA

[b]Institute of Imaging Science, Vanderbilt University, Nashville, TN, USA

[c]Department of Radiology and Radiological Sciences, Nashville, TN, USA

[d]Department of Biomedical Engineering, Vanderbilt University, Nashville, TN, USA

[e]Vanderbilt Ingram Cancer Center, Vanderbilt University, Nashville, TN, USA

[f]Vanderbilt Institute of Chemical Biology, Nashville, TN, USA

[g]Vanderbilt Brain Institute, Vanderbilt University, Nashville, TN, USA

[h]Molecular Physiology and Biophysics, Vanderbilt University, Nashville, TN, USA

Abstract

Polylysine (PL) has been used to facilitate dendritic cell (DC) uptake of super paramagnetic iron oxide (SPIO) nanoparticles for use in magnetic resonance imaging (MRI). In this work, we examined the effect of PL on cell toxicity and induction of cell maturation as manifested by the up-regulation of surface molecules. We found that PL became toxic to bone marrow-derived DCs (BMDCs) at the 10 μg/ ml threshold. Incubation of BMDCs with 20 μg/ml of PL for 1 h resulted in approximately 90% cell death. However, addition of SPIO nanoparticles rescued DCs from PL-induced death as the combination of SPIO with PL did not cause cytotoxicity until the PL concentration was 1000 μg/ml. Prolonged exposure to PL induced BMDC maturation as noted by the expression of surface molecules such as MHC class II, CD40, CCR7 and CD86. However, the combination of SPIO and PL did not induce BMDC maturation at 1 h. However prolonged exposure to SPIO nanoparticles induced CD40 expression and protein expression of TNFα and KC. The data suggest that the use of PL to enhance the labeling of DCs with SPIO nanoparticles is a dedicated work. Appropriate calibration of the incubation time and concentrations of PL and SPIO nanoparticles is crucial to the development of MRI technology for noninvasive imaging of DCs in vivo.

*Corresponding authors: W. Pham is to be contacted at Institute of Imaging Science, Vanderbilt University School of Medicine, Nashville, TN 37232-2310. S. Peebles, Division of Allergy, Pulmonary and Critical Care Medicine, Vanderbilt University School of Medicine, Nashville, TN 37232-2650. stokes.peebles@Vanderbilt.Edu (R.S. Peebles), wellington.pham@vanderbilt.edu (W. Pham).

Keywords

Iron oxide nanoparticles; Dendritic cells; Polylysine; Transfection; Nanotechnology

Dendritic cells (DCs) are a subset of professional antigen-presenting cells (APCs). They have the ability to process and present antigens via major histocompatibility complex (MHC) molecules for recognition by naïve T-lymphocytes.[1] DCs have multiple roles and dynamically shift phenotypes relative to their task and environment.[2] For instance, while immature DCs are unable to activate T lymphocytes, they reside in tissues that are in contact with the external environment, and provide surveillance for antigens in the epithelia of the skin, the gastrointestinal track, and the respiratory system. Upon encountering the “danger” signals, DCs undergo a differentiation and maturation process manifested by the upregulation of MHC-II and costimulatory molecules CD80 and CD86, which are among the key regulatory factors needed to induce T lymphocyte stimulation. As the most potent APCs, DCs are capable of presenting tumor antigens and effectively stimulating the immune response targeting against a tumor.[3] Because they serve as essential constituents of the immune system to trigger immune reactions, DCs are therefore considered to be promising tools for immunotherapy. Despite its appeal, however, several limitations exist in the use of antigen-pulsed DCs in cell therapy.[4] A key question in DC-based therapy that has yet to be consistently answered is the cellular fate of the cells after injection. To track this dynamic event, a number of imaging modalities have been employed both in mice and humans such as scintigraphy and single-photon-emission computed tomography (SPECT),[5–9] positron emission tomography (PET)[10,11] and magnetic resonance imaging (MRI).[4,12,13] Since DCs are terminally differentiated cells, MRI tracking of DCs using iron oxide nanoparticles offers advantages over scintigraphy and PET in terms of resolution and the intrinsic anatomical feature associated with the technique.

To enable MR imaging of DC migration, the cells are isolated and pulsed with superparamagnetic iron oxide (SPIO) nanoparticles in a cell culture dish. Immature DCs use pinocytosis and phagocytosis to acquire antigen, and so they can take up nanoparticles spontaneously over an extended incubation time. However, shorter incubation times reflect low and insufficient cellular internalization of nanoparticles. Thus, to control cell uptake in particular applications, such as studying mature DCs at which stage DCs have a weak uptake capability, transfection reagents including polyethyleneimine (PEI)[14,15] and polylysine (PL)[4,16] were attached or added to the particles independently during the incubation process to ensure appropriate probe internalization within the DCs to facilitate imaging. Quantitative studies have demonstrated that DCs take up about 10 pg of iron per cell.[12] In the presence of transfection reagents, however, this uptake can increase as high as 35 pg iron per cell.[4,17] Nevertheless, it remains unclear whether the SPIO nanoparticles or transfection reagents or the combination of these two materials play any role in activating DCs or in their viability.

We report here that incubating BMDCs with PL, regardless of the duration of incubation, results in cell toxicity when the 10 μg/ml threshold is reached. In contrast, dextran-coated SPIO nanoparticles are nontoxic to BMDCs regardless of exposure time and concentration. We also found that SPIO nanoparticles significantly reduced PL-induced toxicity when both

were co-incubated with BMDCs. Furthermore, 20 μg/ml PL significantly induced BMDC maturation as manifested by the expression of costimulatory molecules. However, we did not observe any registered release of cytokines caused by PL. On the other hand, SPIO nanoparticles provoke a significant release of cytokines at high concentration (1000 μg/ml), particularly during long periods of incubation. Using cell sorting analysis, we observed the upregulation of costimulatory molecules on BMDCs as a result of PL incubation. SPIO nanoparticles did not induce BMDCs maturation after 1 h of incubation and reduce the PL-induced expression of costimulatory molecules. Alternatively, the preincubation of an appropriate ratio of SPIO:PL before being exposed to DCs enhanced SPIO nanoparticle uptake in immature BMDCs. These data suggest the possibility of maintaining the pristine function and viability of BMDCs after enhancing their uptake of SPIO nanoparticles using PL, albeit with careful calibration.

Methods

Materials

General chemicals were of the best grade available, supplied by Sigma Aldrich (St. Louis, MO). Dextran-coated SPIO nanoparticles were developed in house as reported elsewhere.[4] PL (99% poly-D-lysine hydrobromide, average molecular weight 30,000–70,000) and dextran (T-10) were purchased from Sigma-Aldrich and GE Healthcare (Waukesha, WI), respectively, used without further purification. Antibodies were purchased from eBioscience(San Diego, CA) and Biolegend (San Diego, CA). CCL19-Fc Fusion Recombinant protein was purchased from eBioscience.

Animals

C57BL/6 mice were obtained from the Jackson Laboratory (Bar Harbor, ME) and bred in house. Animal experiments were carried out per the guidelines provided by the Vanderbilt University Institutional Animal Care and Use Committee and the National Institutes of Health Guide for the Care and Use of Laboratory Animals.

Isolation of BMDCs

BMDCs were isolated from mouse bone marrow, as described, with slight modifications.[4] Briefly, bone marrow cells in the femurs and tibias of mice were flushed out with RPMI1640 medium (Life Technology/Invitrogen, Grand Island, NY), using a 1 ml syringe incorporating a 27-gauge needle (BD Biosciences, San Jose, CA). The cells were collected into a 50 ml conical tube after being passed through a 70 μm pore sized nylon mesh cell strainer (BD Biosciences, San Jose, CA). The red cells were removed from the bone marrow cells with 3 min of incubation time in 0.83% ammonium chloride at room temperature, followed by two washes with RPMI1640 medium. The remaining bone marrow cells were counted and cultured in 6-well plates (Costar, Corning, NY,) at a density of 1×10^6 cells/ml. The RPMI 1640 medium used for BMDC preparation was supplemented with 5% fetal bovine serum (FBS), 55 nM of 2-mercaptoethanol, 50 μg/ml gentamicin and 20 ng/ml recombinant murine granulocyte macrophage colony stimulating factor (GM-CSF) (PeproTech, Rocky Hill, NJ). New medium containing GM-CSF was added to each plate on

day 3 of culture. On day 6, weakly attached cells were collected and used for experiments as immature BMDCs.

BMDC survival analysis

Cell death was measured with propidium iodide (PI) staining by flow cytometry. After treatment with PL, SPIO nanoparticles, dextran T-10, both PL and SPIO nanoparticles or both PL and dextran T-10, the BMDCs were stained with fluorescently-labeled antibodies. PI was then added to the stained cells 10 min before measurement by flow cytometry. Cell viability was calculated as the ratio of PI-negative gated cells excluding cell debris gating. Measurements were performed four times and the average measurement is presented. All data were expressed as mean ± SE for quadruplicate.

Cytotoxicity caused by PL, SPIO nanoparticles or the combination of PL and SPIO nanoparticles was determined by the MTT and LDH assays. Briefly, after treatment with various concentrations of PL and SPIO for 12 h, the plates were centrifuged at 1000 rpm for 10 min, after which 100 μl of the supernatant was transferred to a new 96-well plate. The LDH in the supernatant was measured with the LDH Cytotoxicity Assay Kit (Cayman Chemical, Ann Arbor, MI) according to the manufacturer's instructions.

For the MTT assay, BMDCs were resuspended in a phenol red-free RPMI 1640 medium (Gibco Life Technologies, Grand Island, NY) which contained 5% FBS and 50 μg/ml gentamicin. The 5×10^4 BMDCs were seeded in 96-well plates, after which a different concentration of PL was added. After 12 h, 10 μl of PBS that contained 5 mg/ml 3-(4,5-dimethyl-2-thiazolyl)-2,5-diphenyl-2H-tetrazolium bromide (MTT) (Molecular Probes, Invitrogen Life Technologies, Grand Island, NY) was added to each well. The plates were then incubated for 4 h at 37 °C in humidified air containing 5% CO_2. Next, 100 μl of SDS-0.01 M HCl solution was added to each well and mixed thoroughly using a pipette. The plates were then incubated for 4 h at 37 °C in humidified air containing 5% CO_2. After the incubation process, absorbance at 570 nm was measured using a VERSAmax™ microplate reader (Molecular Devices, Downingtown, PA).

Cell surface phenotyping

The phenotype of BMDCs, after treatment with PL, SPIO nanoparticles, dextran T-10, both PL and SPIO nanoparticles or both PL and dextran T-10, was analyzed using a BD LSRII flow cytometer (BD Biosciences) and FlowJo software (Tree Star, Ashland, OR) at the Vanderbilt Flow Cytometry Core laboratory. The cells were pretreated with affinity-purified anti-mouse CD16/CD32 monoclonal antibody (eBioscience) to block any nonspecific antibody binding. For each set of staining groups, 1.0×10^6 cells were incubated at 4 °C for 45 min with monoclonal antibodies in 3% FBS containing PBS. They were then washed twice with 3% FBS containing PBS after which PI was added. A total of 10,000 live $CD11c^+$ cell events as gated on PI negative and CD11c positive fractions were acquired and analyzed. The monoclonal antibodies used for BMDC surface staining were as follows: Alexa Fluor-700 anti-mouse major histocompatibility complex (MHC) class II antibody (Biolegend); fluorescein isothiocyanate (FITC) anti-mouse CD40 antibody (Biolegend); and phycoerythrin (PE)-Cy7 anti-mouse CD86 antibody (B7-2; Biolegend). Isotypic control

antibodies were used as negative controls. Mouse CCL19-Fc fusion recombinant protein and PE anti-human IgG antibody (eBioscience) were used for CCR7 staining. PE anti-human IgG antibody was used only as a negative control for CCR7 staining.

Cytokine measurements

Proinflammatory chemokine and cytokine (KC and TNFα) levels in culture supernatants of BMDCs treated with PL, SPIO nanoparticles or both for periods of 1 h and 12 h were measured using Duoset ELISA kits (R&D Systems, Minneapolis, MN) according to the manufacturer's instructions. To assess SPIO nanoparticles interference during the ELISA procedure, culture supernatants of BMDC treated with LPS (1 μg/ml) for 24 h were added to 96-well ELISA plates with increasing concentrations of SPIO nanoparticles. After a 2-h incubation period, the supernatants were aspirated and the wells washed three times with buffer before measurement using manufacturer's instructions. Values below the detection limit were assigned half the value of the lowest detectable standard.

Coating the SPIO nanoparticles with PL

SPIO nanoparticles (10 mg/ml) were treated with PL (200 μg/ml) for 3 h at room temperature, and SPIO nanoparticles coated with PL were isolated by using a magnetic-activated cell sorting (MACS) column (Miltenyi Biotech) to remove any remaining PL. The concentration of the coated product was then quantified using inductively coupled plasma mass spectrometry (ICP-MS).

Uptake and quantitative analysis of cellular-associated SPIO nanoparticles

The uptake of SPIO nanoparticles was confirmed via Prussian blue staining of the cytospin preparations. Initially, 1.0×10^6 BMDCs were treated with SPIO nanoparticles, SPIO nanoparticles coated with PL or mixture of SPIO nanoparticles and PL which was immediately added to cell suspension after the preparation was mixed. The cells treated with each condition were washed twice with PBS to remove any remaining SPIO and PL. For Prussian blue staining, an aliquot comprised of 200 μl of DCs (2×10^5 cells) in PBS with 10% serum was pelleted onto each slide. The slides were dried at room temperature and fixed with 10% formalin for 10 min. The samples were then stained with a freshly mixed solution of 10% hydrochloric acid and 5% potassium ferrocyanide solution for 20 min. After three washes with water, the slides were counterstained with 0.1% nuclear fast red for 5 min. After another rinse with water, the slides were dehydrated with 95% and 100% ethanol, and then were observed under a microscope.

Quantitative analysis of the Prussian blue signal expressed within the DCs was conducted using MATLAB (MathWorks, Inc., USA). An analysis protocol was developed to quantify the signal in each cell via imaging analysis that focused on segmenting the positive (blue colored) area of the staining. RGB images of the stained cells were analyzed to identify positively stained areas where intensities in the blue channel were at least 10% greater than the others two channels. The percentage of the positive area to the local cell area, which was segmented using similar methods.

Transmission electron microscopy

Immature BMDCs were co-incubated with 1000 μg/ml of SPIO nanoparticles and with 20 μg/ml or without PL for 1 h. The SPIO-labeled BMDCs were collected and then fixed with 2.5% glutaraldehyde and 0.1-M sodium cacodylate for 1 h. The sample was then rinsed with sodium cacodylate (twice, 5 min for each wash), followed by a second fixing with 1% osmium tetroxide for 1 h. The sample was rinsed several times with 50%, 70%, 95%, and 100% ethanol and then with 50% and 100% propylene oxide. The samples were then dehydrated and filtered onto an Epon 812 resin-coated copper grid. The sections were imaged on a Philips CM 12 microscope.

Statistical Analysis

Data were expressed as means ± SE. The statistical significance of the differences between sample means was determined via Dunn's multiple comparison test administered following the Kruskal–Wallis (nonparametric ANOVA) test, the results of which were considered significant when $P < 0.05$ as reported with GraphPad Prism software.

Results

Viability of BMDCs upon exposure to PL or/and SPIO nanoparticles

To elucidate the effect of the transfection reagent on cell survival, immature BMDCs (1.0×10^6 cells/ml) were incubated with various concentrations of PL for periods of 1 or 12 h. After incubation the cells were washed three times with PBS before being exposed to PL and undergoing cell sorting analysis. Treatment of BMDCs with PL 1.25 μg/ml or 2.5 μg/ml did not increase cell death at 1 or 12 h compared to vehicle-treated BMDCs (Figure 1, *A*). At 5 μg/ml, there was no significant difference in the induction of cell death in the BMDCs at 1 h or 12 h compared to vehicle. However, there was a statistically significant 50%–60% cell death at the PL 10 μg/ml concentration compared to the vehicle ($P < 0.05$) and approximately 90% cell death at the PL 20 μg/ml concentration. Using MMT assay we established a dose–survival curve and calculated the LD_{50} for PL at 12 h of incubation. The data corroborated with the observation pointed out in Figure 1, *A* that the LD_{50} of PL for BMDCs is approximately 10–12 μg/ml (Supplementary data, Figure S1). Furthermore, we confirmed the cell toxicity of PL by LDH assay, since the LDH release in this assay is measured as a consequence of cell membrane destruction. As anticipated, the LD_{50} for PL from the LDH assay is approximately the same as observed in MTT assay (Supplementary data, Figure S1). Taken together, the result obtained from both procedures indicated that PL induced cell death in a dose-dependent fashion. These supplementary data testified propriety of measurement in Figure 1, *A*.

We incubated BMDCs with SPIO nanoparticles at concentrations sufficient to produce contrasting signals in MR imaging. No cell death was registered 1 and 12 h after incubation with SPIO nanoparticles compared to the vehicle (Figure 1, *B*). This indicates that SPIO nanoparticles are nontoxic for immature BMDCs.

Our group and other investigators have previously shown that there was no cell toxicity when PL and SPIO nanoparticles were combined in cell uptake assays[4,16]; however, the

dose of SPIO nanoparticles necessary for the protective effect has not been defined. Therefore, we sought to determine the minimum concentration of SPIO nanoparticles necessary for prevention of cell death from PL. We co-incubated BMDCs with the highest dose of PL (20 μg/ml) performed in the last assay and with different concentrations of SPIO nanoparticles. To make the comparison as objectively analytical as possible, the assay was performed under conditions similar to those present in other assays, shown in Figure 1, *A* and *B*, including incubation time. Figure 1, *C* showed that SPIO nanoparticles improved cell survival even at a dose as low as 20 μg/ml. Beginning at the 200 μg/ml threshold, SPIO nanoparticles were able to restore cell normality despite the presence of PL ($P < 0.05$, both 1 and 12 h of incubation). This protection phenomenon of SPIO nanoparticles was also observed with higher doses, up to 400 μg/ml. However, we observed a small BMDC toxicity when the concentration of SPIO nanoparticles increases to 1000 μg/ml.

The effect of PL or/and SPIO nanoparticles on BMDC maturation

To determine whether immature BMDCs were activated upon uptake of PL or SPIO nanoparticles, we performed cell sorting analysis to assess the molecular biomarkers of BMDC maturation such as CD86, CD40, CCR7 and MHC-II. Figure 2, *A* illustrates that PL did not induce BMDC maturation at low concentration and during short incubation time. However, it became apparent that CD40 expression was significantly upregulated with 20 μg/ml of PL after one hour of incubation. When the concentration increased from the 10 μg/ml threshold, PL induced the upregulation of several key costimulatory molecules, such as CD86, CCR7 and MHCII; however, this typically occurred after a protracted incubation time (Figure 2, *D*). In contrast, the SPIO nanoparticles did not induce BMDC maturation even at a high concentration (1000 μg/ml) during short incubation time (Figure 2, *B*). We observed CD40 expression by SPIO nanoparticles at high concentration, but only when the incubation duration was 12 h ($P < 0.05$) (Figure 2, *E*). We also observed further that if BMDCs were exposed to PL and SPIO nanoparticles simultaneously, any increase in the concentration of SPIO nanoparticles, even from a small dose, dampened the effect of PL on BMDC maturation (Figure 2, *C* and *F*). Co-incubation of 20 μg/ml PL with SPIO at 100 μg/ml and 200 μg/ml significantly decreased co-stimulatory molecule expression compared to co-incubation with 20 μg/ml PL and vehicle.

The effect of dextran T-10 on BMDC viability and maturation

Since the outer surface of the SPIO nanoparticles was coated with dextran,[4] we wished to determine if cell viability or activation of cell maturation manifested by the upregulation of costimulatory molecules, could be attributed to the dextran. Toward that end, immature BMDCs were treated with varying concentrations of dextran T-10 for 12 h, after which they were subjected to cell sorting analysis comparing to the vehicle. Figure 3, *A* shows that BMDCs treated with dextran T-10, even at high concentrations (2000 μg/ml), did not affect cell viability. Further, there is no up-regulation of cell surface-expressed costimulatory molecules upon exposure to dextran T-10 (Figure 3, *B*). These results imply that dextran did not induce BMDC maturation. In contrast to the observation that SPIO nanoparticles have the ability to rescue BMDCs from the toxicity caused by PL, dextran T-10 is inert in that regard (Figure 3, *C*). In contrast to what was seen with the SPIO nanoparticles, dextran

polymer had no impact on the levels of expression of costimulatory molecules in the presence of PL (Figure 3, *D*).

The effect of PL or/and SPIO nanoparticles on cytokine production from BMDCs

The next relevant task was to determine if DCs produce mediators such as cytokines in response to PL or/and SPIO nanoparticles exposure. We performed ELISA assays to measure the proinflammatory chemokine and cytokine expression after incubation of BMDCs with PL or SPIO nanoparticles or both. Despite inducing BMDC maturation as evidenced by the up-regulation of several costimulatory molecules on the cell surface, PL did not stimulate the release of cytokines from the BMDCs (Figure 4). ELISA analysis indicated that the levels of KC and TNFα after incubation at a high PL concentration produced an insignificant amount of cytokines compared to the vehicle group after 1 h of incubation. A very small amount of cytokines was released over a prolonged incubation time, and the same result was observed for the low dose SPIO nanoparticles. Surprisingly, incubating BMDCs with a high concentration of SPIO nanoparticles (1000 μg/ml) stimulated a remarkable release of both KC and TNFα. Of note, this trend is identical to the conditions when BMDCs were co-incubated with SPIO nanoparticles and PL. We decided to investigate further whether the BMDCs' cytokine release was induced by dextran T-10 which is the coating material on the surface of SPIO nanopartilces. However, we observed that the polymer caused no effect on KC and TNFα release after BMDCs were treated with various concentrations of dextran T-10 (10–2000 μg/ml) (data not shown).

The effect of PL on SPIO nanoparticles uptake by immature BMDCs

We examined the effect of mixing versus coating dextran-coated SPIO nanoparticles with PL. As shown in Figure 5, treating immature BMDCs with a mixture of SPIO and PL caused a significant increase in SPIO nanoparticles uptake (Figure 5, *C*-*E*) compared to treating the cells with only SPIO nanoparticles. In addition, we observed that coating SPIO nanoparticles with PL proved to be a much more effective delivery approach (Figure 5, *D*). The data obtained in the quantitative analysis (Figure 5, *F*) demonstrated that coating the nanoparticles resulted in a twofold improvement in cell uptake compared to mixing SPIO with PL prior to cell exposure (Figure 5, *C* versus *D* and quantitative analysis *F*). Notably, however, the process of coating dextran-coated SPIO with PL is extremely rapid. Our previous publication reported that such coating process would take no more than 15 min.[18] Yet the data obtained from this work suggest that the uptake is dependent on the ratio of SPIO nanoparticles to PL to a certain extent. We noted that a mixture comprised of a high concentration of PL (20 μg/ml) and low concentration of SPIO nanoparticles (100 μg/ml) was more effective than the reverse (Figure 5, *E* versus *C*). Taken together, PL significantly increased SPIO nanoparticle uptake by BMDCs in a dose-dependent fashion, and coating the nanoparticles by brief preexposure to PL appears to be the ideal approach.

Evidence of SPIO-laden BMDCs by Transmission Electron Microscopy

TEM confirmed the results obtained from Prussian blue staining data, such that PL improved cell uptake after 1 h of incubation (Figure 5, *G* & *H*). Further, it provides remarkable resolution that the internalized SPIO nanoparticles had been detected in the

endosomal vesicles of the DCs (arrows). Since the iron cores of the SPIO nanoparticles have an average diameter of approximately 10 nm,[4] the TEM portrayed them as tiny, dark dots. In most cases, the nanoparticles cluster into colonies. In BMDCs treated with PL and SPIO, a greater number of dark dot clusters were observed in the cytoplasm. This outcome is consistent with the data indicated by Prussian blue staining.

Discussion

Global tracking of the distribution of adaptively transferred DCs is of paramount importance in cell therapy. Imaging DCs using MRI provides good spatial resolution, including exquisite dynamic information and anatomical contrast, among the non-invasive modalities.[1] Currently, T2-mediated MR imaging using SPIO nanoparticles is a preferred technique given its clinical relevance. To enable this, DCs are isolated and pulsed with SPIO nanoparticles in a cell culture dish before being injected into the host. DCs are capable of uptake of nanoparticles, especially immature cells have demonstrated efficient nanoparticle uptake capability. However, since the process is time dependent, a transfection agent, such as PL was utilized to enhance the cell uptake of nanoparticles for short duration incubation. Although labeling DCs with SPIO nanoparticles and PL is not new, the relative DC tolerance dose when exposed to each material is largely unknown. Since imaging is subordinate to the primary therapy objective, it is necessary to optimize cell labeling methods to ensure (i) labeling reproducibility, (ii) that labeled cells retain their functional viability and (iii) that the process does not perturb to the target cells.[19] To that end, our study aimed to analyze the implication of PL and SPIO nanoparticles on DC during brief and extended period of incubation. The SPIO nanoparticles were developed and reported previously.[4] These nanometer-sized iron oxide particles were coated with dextran, resulting in an overall size of 30 nm. The material was used for T2-weighted and T2*-weighted imaging due to shortening of T2 and T2* relaxation times. Upon beginning the experiment, we did not anticipate that PL treatment would cause significant toxicity and facilitate BMDCs' up-regulation of costimulatory molecules. In the past, we incubated DCs with SPIO nanoparticles and PL up to the 20 μg/ml concentration threshold without noting any registered cell death.[4] In this experiment, however, the same concentration of PL alone was responsible for nearly 90% of cell death upon exposure in 1 h of incubation ($P < 0.05$) (Figure 1, *A*). Cell death became even more severe when PL exposure time was extended. In contrast, SPIO nanoparticles caused neither toxicity nor cell death (Figure 1, *B*). The most critical observation noted in this experiment is the implication of PL in the BMDC maturation process. However, low doses have no effect on BMDC maturation. These data demonstrate that PL acts as a double-edge sword, such that depending on the concentration used, the compound can be either safe or toxic. Moreover, PL induced the up-regulation of costimulatory molecules (Figure 2, *A* and *D*), the process may interfere with research that focused on the regulation of phenotypical maturation or DC migration. During the course of this work, we noted a report by Strand et al[20] that PL caused substantial monocyte cell death at concentrations higher than 10 μg/ml. This observation is generally consistent with our work although these researchers used monocytes in their approaches. Further, this group also suggested that PL may provoke an inflammatory response at high concentrations by releasing proinflammatory cytokine, tumor necrosis factor (TNF).

To assess the viability of BMDCs in the presence of SPIO nanoparticles and PL, we chose the highest concentration of PL from the previous assay. As shown in Figure 1, *C*, PL causes more than 90% of cell death at this dose. Adding SPIO nanoparticles, beginning at the 40 μg/ml concentration threshold in the presence of supposedly toxic levels of PL, led to remarkably improved cell viability. This phenomenon was also consistently observed at higher SPIO nanoparticle doses. To explain the reason why SPIO nanoparticles rescue the toxicity caused by PL, we think that the anionic dextrane polymer coated on the surface of SPIO nanoparticles might play a role to block or reduce the toxicity effect from PL through electrostatic interaction. Our observation is supported by a report that described polyanions, such as polyglutamate, pentosan polysulphate or heparin can effectively neutralize the charge from PL and thus abolish its cytotoxic effects.[21] Except at 1000 μg/ml of SPIO nanoparticles, BMDC viability began to decline. Although our results do not necessarily explain the mechanism by which SPIO nanoparticles thwart the toxicity generated by PL, we speculate that nanoparticles may protect BMDCs from PL-generated toxicity by shielding the positive charge groups via an electrostatic interaction as we observed in a similar case previously.[18]

In another set of experiments, we sought to evaluate the influence of SPIO nanoparticles on BMDC maturation based on the up-regulation of cell surface molecules caused by PL. We noted with interest a marked reduction in maturation of PL-treated BMDCs as the concentration of SPIO nanoparticles was increased. At the 40 μg/ml threshold, SPIO nanoparticles prevented PL-induced BMDC surface expression of MHC class II, CD 40, CCR7, CD86, thus maintaining an immature BMDC phenotype (Figure 2, *C* and *F*). After combining this outcome with data acquired during our preceding experiment, we observed that cell viability was restored at the 40 μg/ml SPIO nanoparticle threshold. This result suggests that the toxicity caused by PL is not associated with cytokines production since none were detected in the culture medium (Figure 4). This observation contrasts with outcome linked with PL-treated monocytes.[20] Although evidence suggests PL-induced uptake of SPIO nanoparticles in both BMDCs[4] and monocytes,[20] no current theory can adequately explain the different levels of cytokine release caused by them. The most interesting observation in this work is that a high concentration of SPIO nanoparticles can provoke BMDCs to release significant amounts of cytokines. While previous studies have shown that low doses of SPIO nanoparticles did not induce cytokine release,[22] no other study has observed a cytokine release in BMDCs treated with high concentrations (such as 1000 μg/ml). This action is independent of PL or dextran T-10. We also confirmed that SPIO nanoparticles did not interfere with cytokine analysis assays (Supplementary data, Figure S2).

Furthermore, we confirmed that PL-mediated BMDCs could uptake of the SPIO nanoparticles (Figure 5). The data obtained from the Prussian blue staining corroborate with those obtained in the past by our group and other investigators, that the uptake of SPIO nanoparticles was increased in the presence of PL.[4,22] In this study, we found two new concepts associated with the utilization of PL. The first of which relates to the ratio in which PL is used. While PL is effective in stimulating uptake in a low dose of SPIO nanoparticles, excess PL induces cell death. The second concept focuses on the preincubation of SPIO and

PL, which is also effective in stimulating the uptake of SPIO nanoparticles but prevents cell death via removing the excess of PL prior to cell treatment. Thus, we have shown that SPIO nanoparticles coated with PL through preincubation were readily uptaken into BMDCs. Since cell membranes are inherently negatively charged, it stands to reason that positively charged materials would facilitate easier uptake. However, dextran-coated SPIO nanoparticles are weakly negatively charged. In contrast, as PL is positively charged, it serves as a transfection agent for the uptake of SPIO nanoparticles by changing their surface charge. Therefore, it appears that a brief preincubation is effective for PL adsorption to the surface of SPIO nanoparticles.

In summary, we reported the optimized conditions under which BMDCs can be labeled without perturbing their function. In contrast to the previous study which reported that PL induced dose-dependent cytotoxicity, we found that either the combination of PL and SPIO or coating SPIO with PL, reduced cell toxicity.[20] Our work demonstrated assays capable of navigating the fine line of SPIO nanoparticles and PL on cell labeling. In fact, BMDCs are safe and unresponsive as long as the PL concentration remains below the 5 μg/ml threshold. While increasing the PL concentration may be toxic, if used to enhance SPIO nanoparticle delivery, then that concentration can be indeed increased since toxicity or cell activation phenomenon is decreased. Not only does our study show that such validation is crucial for labeling DCs in therapy, but it also demonstrates the utility of other DC-based research and for other cell types. Further, the data also demonstrate that dextran-coated SPIO nanoparticles are not only biocompatible, but they can also improve cell survival.

Supplementary Material

Refer to Web version on PubMed Central for supplementary material.

Acknowledgments

This work is supported by grants from R01 HL 090664 (R.S.P.), R01 Al 070672 (R. S. P.), R01 Al059108 (R. S. P.), R21 HL 106446 (R. S. P.), U19Al095227 (R. S. P.), Veteran Affairs-1l01BX000624 (R. S. P.) and R01 CA160700 (W. P.), P50 CA128323 (J.C.G) and VICC Cancer Center Support Grant (W. P.) and R01 CA159178 (R. O.).

References

1. Pham W, Kobukai S, Hotta C, Gore JC. Dendritic cells: therapy and imaging. Expert Opin Biol Ther. 2009; 9:539–64. [PubMed: 19392575]
2. Grolleau, A.; Sloan, A.; Mule, JJ. Dendritic cell-based vaccines for cancer therapy. In: Samir, Khleif, editor. Tumor immunology and cancer vaccines. 2005. p. 181-205.
3. Mohty M, Olive D, Gaugler B. Leukemic dendritic cells: potential for therapy and insights towards immune escape by leukemic blasts. Leukemia. 2002; 16:2197–204. [PubMed: 12399962]
4. Kobukai S, Baheza R, Cobb JG, Virostko J, Xie J, Gillman A, et al. Magnetic nanoparticles for imaging dendritic cells. Magn Reson Med. 2010; 63:1383–90. [PubMed: 20432309]
5. Kupiec-Weglinski JW, Austyn JM, Morris PJ. Migration patterns of dendritic cells in the mouse. Traffic from the blood, and T cell-dependent and -independent entry to lymphoid tissues. J Exp Med. 1988; 167:632–45. [PubMed: 3258009]
6. Morse MA, Coleman RE, Akabani G, Niehaus N, Coleman D, Lyerly HK. Migration of human dendritic cells after injection in patients with metastatic malignancies. Cancer Res. 1999; 59:56–8. [PubMed: 9892184]

7. Quillien V, Moisan A, Carsin A, Lesimple T, Lefeuvre C, Adamski H, et al. Biodistribution of radiolabelled human dendritic cells injected by various routes. Eur J Nucl Med Mol Imaging. 2005; 32:731–41. [PubMed: 15924229]
8. Ridolfi R, Riccobon A, Galassi R, Giorgetti G, Petrini M, Fiammenghi L, et al. Evaluation of in vivo labelled dendritic cell migration in cancer patients. J Transl Med. 2004; 2:27. [PubMed: 15285807]
9. Suda T, Callahan RJ, Wilkenson RA, van Rooijen N, Schneeberger EE. Interferon-gamma reduces Ia + dendritic cell traffic to the lung. J Leukoc Biol. 1996; 60:519–27. [PubMed: 8864137]
10. Adonai N, Nguyen KN, Walsh J, Iyer M, Toyokuni T, Phelps ME, et al. Ex vivo cell labeling with 64Cu-pyruvaldehyde-bis(N4-methylthiose-micarbazone) for imaging cell trafficking in mice with positron-emission tomography. Proc Natl Acad Sci USA. 2002; 99:3030–5. [PubMed: 11867752]
11. Olasz EB, Lang L, Seidel J, Green MV, Eckelman WC, Katz SI. Fluorine-18 labeled mouse bone marrow-derived dendritic cells can be detected in vivo by high resolution projection imaging. J Immunol Methods. 2002; 260:137–48. [PubMed: 11792384]
12. de Vries IJ, Lesterhuis WJ, Barentsz JO, Verdijk P, van Krieken JH, Boerman OC, et al. Magnetic resonance tracking of dendritic cells in melanoma patients for monitoring of cellular therapy. Nat Biotechnol. 2005; 23:1407–13. [PubMed: 16258544]
13. Dekaban GA, Snir J, Shrum B, de Chickera S, Willert C, Merrill M, et al. Semiquantitation of mouse dendritic cell migration in vivo using cellular MRI. J Immunother. 2009; 32:240–51. [PubMed: 19242376]
14. McBain SC, Yiu HHP, El Haj A, Dobson J. Polyethyleneimine functionalized iron oxide nanoparticles as agents for DNA delivery and transfection. J Mater Chem. 2007; 17:2561–5.
15. Steitz B, Hofmann H, Kamau SW, Hassa PO, Hottiger MO, von Rechenberg B, et al. Characterization of PEI-coated superparamagnetic iron oxide nanoparticles for transfection: size distribution, colloidal properties and DNA interaction. J Magn Magn Mater. 2007; 311:300–5.
16. Arbab AS, Bashaw LA, Miller BR, Jordan EK, Lewis BK, Kalish H, et al. Characterization of biophysical and metabolic properties of cells labeled with superparamagnetic iron oxide nanoparticles and transfection agent for cellular MR imaging. Radiology. 2003; 229:838–46. [PubMed: 14657318]
17. Foster PJ, Dunn EA, Karl KE, Snir JA, Nycz CM, Harvey AJ, et al. Cellular magnetic resonance imaging: in vivo imaging of melanoma cells in lymph nodes of mice. Neoplasia. 2008; 10:207–16. [PubMed: 18320065]
18. Mackay PS, Kremers GJ, Kobukai S, Cobb JG, Kuley A, Rosenthal SJ, et al. Multimodal imaging of dendritic cells using a novel hybrid magneto-optical nanoprobe. Nanomedicine. 2011; 7:489–96. [PubMed: 21215329]
19. Frank JA, Anderson SA, Kalsih H, Jordan EK, Lewis BK, Yocum GT, et al. Methods for magnetically labeling stem and other cells for detection by in vivo magnetic resonance imaging. Cytotherapy. 2004; 6:621–5. [PubMed: 15773025]
20. Strand BL, Ryan TL, In't Veld P, Kulseng B, Rokstad AM, Skjak-Brek G, et al. Poly-L-Lysine induces fibrosis on alginate microcapsules via the induction of cytokines. Cell Transplant. 2001; 10:263–75. [PubMed: 11437072]
21. Morgan DM, Clover J, Pearson JD. Effects of synthetic polycations on leucine incorporation, lactate dehydrogenase release, and morphology of human umbilical vein endothelial cells. J Cell Sci. 1988; 91(Pt 2):231–8. [PubMed: 3267696]
22. Richards JM, Shaw CA, Lang NN, Williams MC, Semple SI, MacGillivray TJ, et al. In vivo mononuclear cell tracking using superparamagnetic particles of iron oxide: feasibility and safety in humans. Circ Cardiovasc Imaging. 2012; 5:509–17. [PubMed: 22787016]

Appendix A. Supplementary data

Supplementary data to this article can be found online at http://dx.doi.org/10.1016/j.nano.2013.05.010.

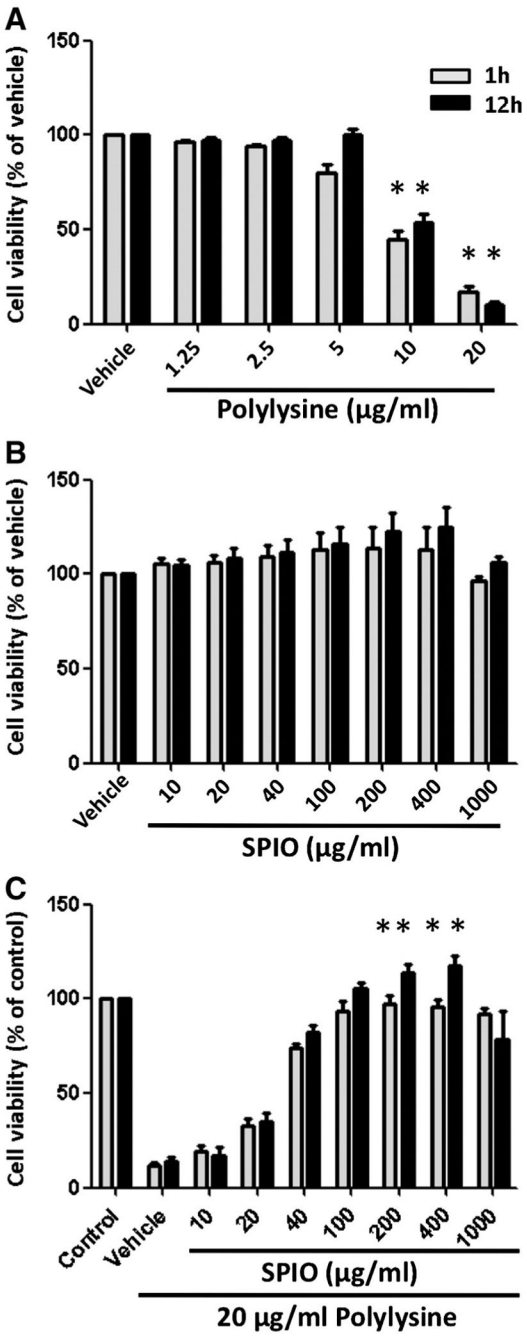

Figure 1.

Viability of BMDCs incubated with PL, SPIO nanoparticle or both. Immature, BMDCs were grown in the absence (vehicle) or presence of increasing concentrations of **(A)** PL, **(B)** SPIO nanoparticles, and **(C)** both PL and SPIO nanoparticles for periods of 1 and 12 h. Control means BMDCs alone. Data were normalized to the vehicle or control. Columns, mean from four experiments; bars, SE. *, Statistical significance ($P < 0.05$), compared with the vehicle or control.

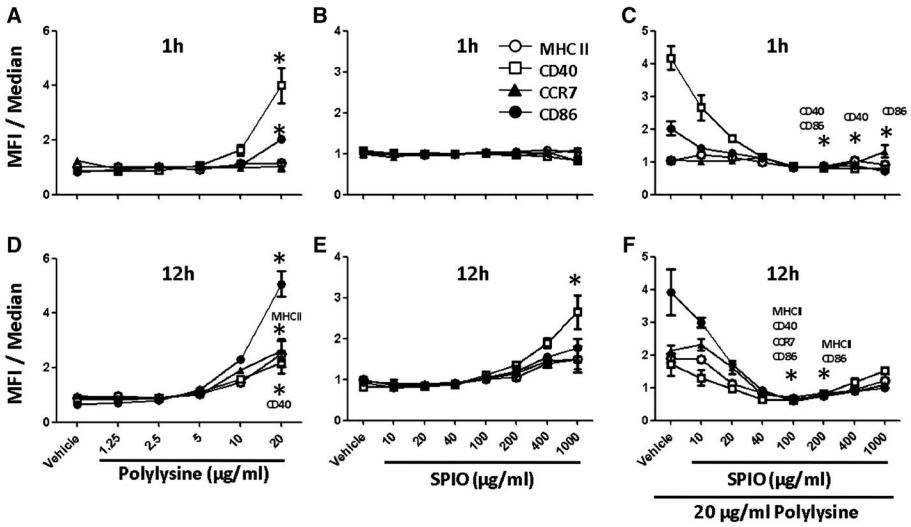

Figure 2.

Cell surface phenotype as determined by flow cytometric analysis of unlabeled BMDCs (vehicle), PL-labeled **(A, D)**, SPIO-labeled cells **(B, E)** or PL-labeled cells in the presence of increasing concentrations of SPIO nanoparticles **(C, F)**. Following 1 and 12 h of incubation with PL, SPIO nanoparticles or both, 1.0×10^6 cells were stained with monoclonal antibodies for antigen presenting receptors MHC-II as well as costimulatory molecules such as CD40, CD86 and chemokine receptor CCR7. Data from the histograms were normalized to the median and compiled into the charts (n = 4 per time point per group). *, Statistical significance $P < 0.05$, compared to the vehicle.

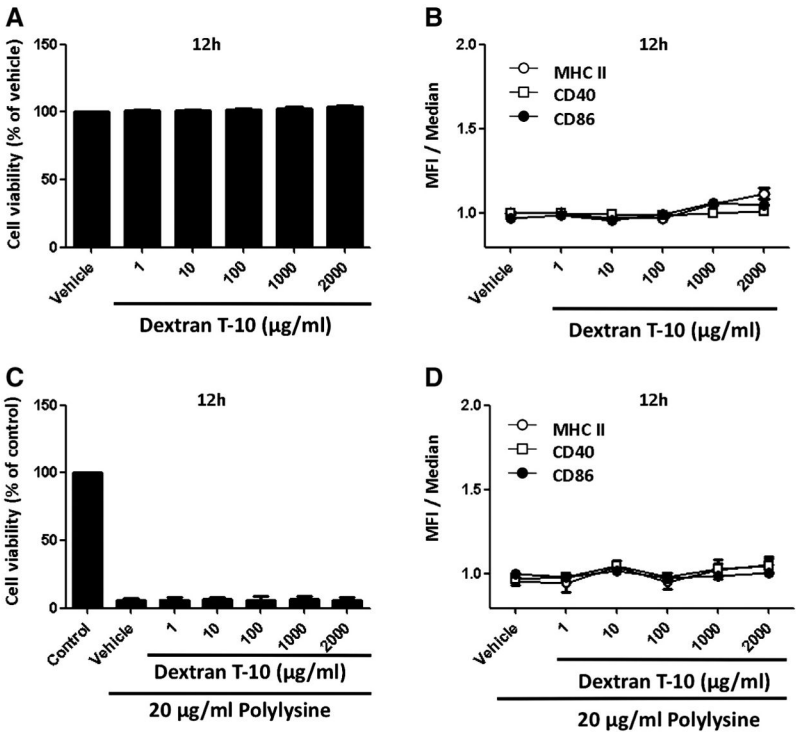

Figure 3.

Viability and cell surface phenotype of BMDCs incubated with dextran T-10 or a combination of PL and dextran T-10. Immature BMDCs were grown in the absence (vehicle) or presence of increasing concentrations of dextran T-10 **(A, B)** or a combination of PL and dextran T-10 for 12 h **(C, D)**. The control was comprised of BMDCs alone. Data that appear in the bar graph were normalized to the vehicle or control. Data that appear in the line graph were normalized to the median. Each value represents the mean from four experiments. Bars represent SE.

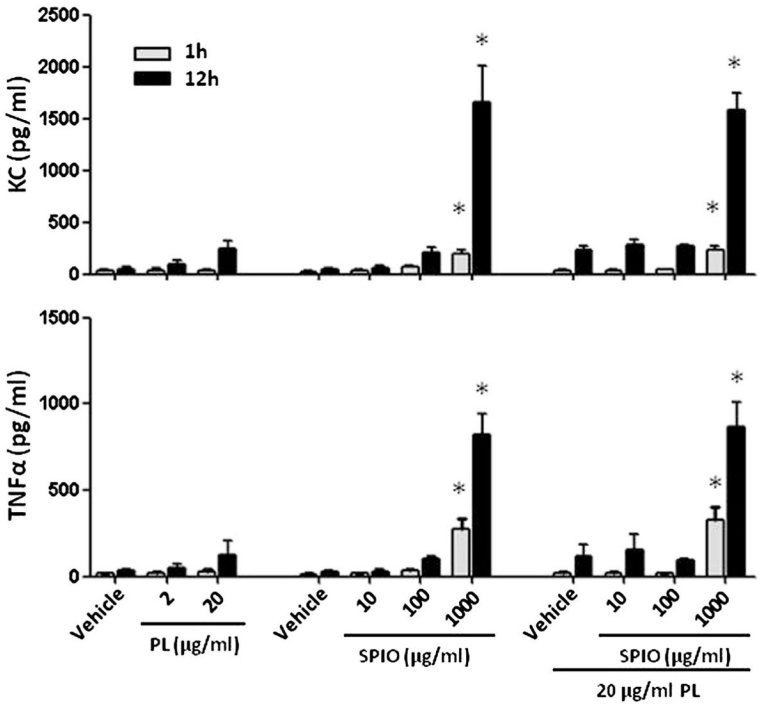

Figure 4.

Analysis of the cytokine profiles in the cell culture medium 1 and 12 h after treating BMDCs with PL, SPIO nanoparticles or both. Each value represents the mean from four experiments. Bars represent SE. *, Statistical significance $P < 0.05$, compared to the vehicle.

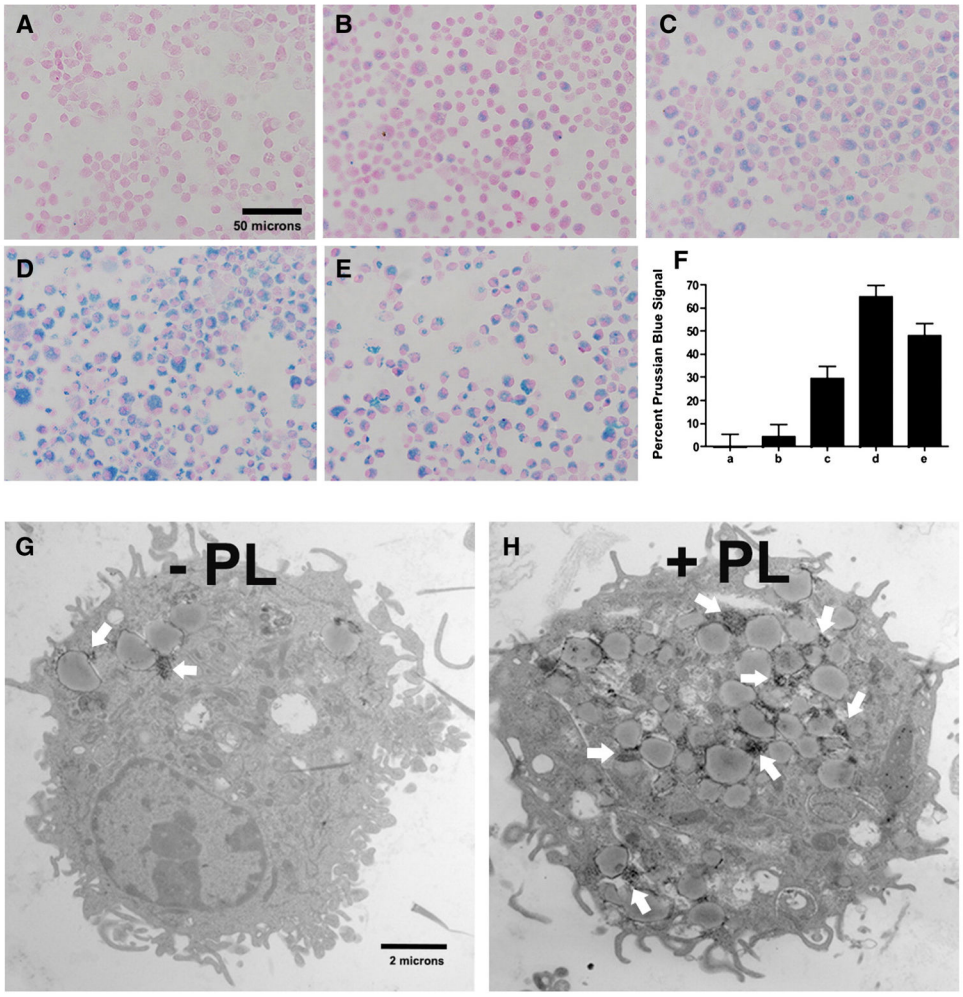

Figure 5.

Prussian blue staining was used to assess the effect of PL-induced internalization of SPIO nanoparticles by immature BMDCs that had been labeled for 12 h (nuclear fast red counterstain; magnification at 600×). Non-labeled BMDCs **(A)**, 500 μg/ml SPIO **(B)**, 500 μg/ml SPIO + 10 μg/ml PL mixture **(C)**, 500 μg/ml SPIO nanoparticles coated with PL during a 3-h preincubation **(D)**, 100 μg/ml SPIO + 20 μg/ml PL mixture **(E)**. Quantitative analysis of the uptake of SPIO nanoparticles shown in **A**, **B**, **C**, **D** and **E** by MATLAB **(F)**. PL-mediated delivery of SPIO nanoparticles was confirmed by TEM. Scale bars 2 μm **(G** and **H)**; * Statistical significance $P < 0.05$.